Title

Deep Learning-Based Modulation Classification for OFDM Systems Without Symbol-Level Synchronization

Authors

Kim, Byungjun
Sathyanarayanan, Venkatesh
Mecklenbräuker, Christoph
et al.

Publication Date

2023-06-10

DOI

10.1109/icasspw59220.2023.10193676

DEEP LEARNING-BASED MODULATION CLASSIFICATION FOR OFDM SYSTEMS WITHOUT SYMBOL-LEVEL SYNCHRONIZATION

Byungjun Kim, Venkatesh Sathyanarayanan*, Christoph Mecklenbräuker†, Peter Gerstoft**

*University of California, San Diego, La Jolla, CA, USA. †TU Wien, Vienna, Austria

ABSTRACT

Deep learning (DL)-based modulation classification of incoherently received orthogonal frequency division multiplexing (OFDM) signals is studied. We propose a novel preprocessing algorithm to build features characterizing the modulation of OFDM signals, which are insensitive to synchronization error. With obtained features, pilot subcarrier indices used for CFO correction may also be estimated. The features obtained with the proposed algorithm are classified with a convolutional neural network (CNN)-based classifier. We have evaluated classification performance with simulated and hardware-generated data. Using these features, the modulation classifier outperforms existing DL-based classifiers which assume symbol-level synchronization with up to 25% classification accuracy performance gain.

Index Terms— Modulation Classification, Deep Learning, OFDM

1. INTRODUCTION

Deep learning (DL) has drawn lots of interest in wireless communications including spectrum sensing [1], channel coding [2], and channel prediction [3]. Complex scenario-by-scenario analysis in wireless communication studies become unnecessary by deploying DL. Recognizing modulation is crucial in spectrum sensing to perceive transmission types. By recognizing modulation with DL, a spectrum sensing detector can obtain essential transmission information without complex signal processing [4].

Orthogonal frequency division multiplexing (OFDM) is widely used in wireless communication protocols like Wi-Fi and 5G. In OFDM signals, message bits are modulated to digital symbols with modulation such as QPSK and the symbols are carried in data subcarriers. To recognize transmission type precisely, the modulation of OFDM signals should be determined. However, the modulation classifier for single-carrier signals [5, 6] cannot be directly applied to OFDM signals due to the OFDM structure. Each transmitted OFDM time sample contains partial information about multiple symbols stacked in the frequency domain. Due to this property, received time-domain IQ samples do not explicitly feature modulation of OFDM signals. Therefore, additional processing is required than taking raw time IQ samples as an input for proper modulation classification of OFDM signals.

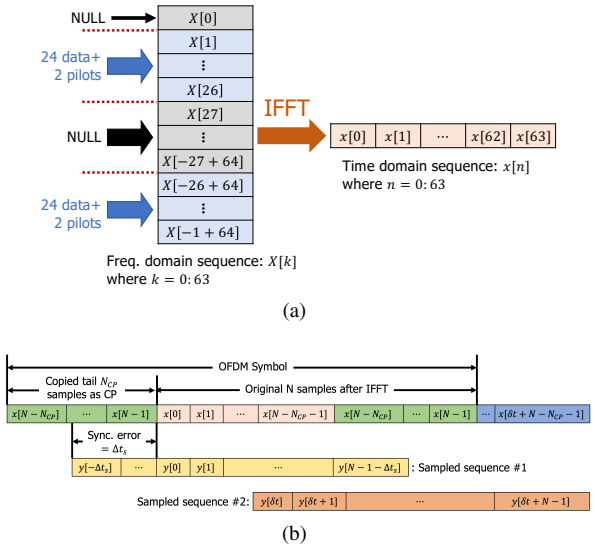

Fig. 1: Generation of OFDM: (a) Conversion of frequency domain symbols to signal samples in time domain and (b) Insertion of CP and sampling sequences.

Different from generic OFDM transmission, spectrum sensing detectors should estimate modulation without detecting preamble. In a Wi-Fi system, preamble makes a receiver (Rx) synchronize with a transmitter (Tx) as well as notifies modulation being used [7]. Thus, for spectrum sensing, OFDM modulation classification needs to be addressed without the assumption of symbol-level synchronization.

In this paper, we propose a novel preprocessing algorithm to build a modulation feature robust to synchronization error, which can be caused by the Rx not knowing exactly when an OFDM symbol starts. Though there have been many efforts to classify modulation of OFDM signals [8], this is the first work to classify modulation of OFDM signals without symbol-level synchronization using DL. We verify that a CNN-based classifier which takes the proposed feature as an input outperforms existing work assuming symbol-level synchronization between a Tx and an Rx. The evaluation has been done with two datasets including hardware-generated data.

The procedure by which OFDM signals are generated is

illustrated in Fig. 1. The parameters in Fig. 1 are from non-high throughput (non-HT) mode OFDM-based Wi-Fi. Fig. 1a describes how time samples carry the information. IFFT is taken over 64 symbols, which consist of 48 data symbols, 4 symbols on pilot subcarriers, and 12 inactive symbols on null subcarriers. Pilot subcarriers are used to estimate residual CFO and sampling rate offset (SRO) [9]. Symbols in OFDM are included in the frequency domain, therefore identifying modulation features from time samples is not straightforward. The CP is appended to the time sequence generated with IFFT, see Fig. 1b. In OFDM systems, the last N_{CP} time samples are copied just before the IFFT sequence to prevent Rx from inter-symbol interference.

CFO occurs when the local oscillator (LO) in the Rx does not synchronize with the carrier in the received signal. This phenomenon has two main causes: frequency mismatch between the Tx and the Rx oscillators and time-variance of the communication channel, e.g. due to Doppler effects. In the presence of CFO, the signal demodulated from the carrier frequency, $y[n]$ is related with $x[n]$ as

$$y[n] = \left(x[n]\mathrm{e}^{j2\pi f_c n T_s}\right) \mathrm{e}^{-j(2\pi(f_c+\Delta f_c)nT_s)} \quad (1)$$

$$= x[n]\mathrm{e}^{-j(2\pi\Delta f_c n T_s)}, \quad (2)$$

where T_s, f_c, and Δf_c denote sampling period, Tx carrier frequency and deviation of Rx carrier frequency from f_c. With constant Δf_c, CFO causes a phase drift which varies linearly over time. In protocol-compliant transmission, Δf_c is estimated using preambles and pilot subcarriers.

2. PROPOSED ALGORITHM

Fig. 1b illustrates the scenario where we sample the sequences. Sequences of length N, the number of subcarriers, are sampled, so they might be contained in a single OFDM symbol (sampled sequence #1) or spans two OFDM symbols (sampled sequence #2). The term OFDM symbol denotes a sequence composed of an IFFT sequence and a CP, and a symbol means a complex number used to carry bits.

The motivating observation for our proposed algorithm is that if a sampled time-domain sequence is contained in a single OFDM symbol, the FFT of that sequence gives the original symbols with phase drift scaling linearly with subcarrier index k

$$Y^i_{\Delta t_s}[k] \triangleq \mathcal{F}\left(y^i[n-\Delta t_s]\right) = \sum_{n=0}^{N-1} y^i[n-\Delta t_s]\mathrm{e}^{-j2\pi nk/N}$$
$$= Y^i[k]\mathrm{e}^{-j2\pi\Delta t_s k/N}, \quad (3)$$

where $Y^i[k]$ denotes the received symbol in subcarrier k of the ith OFDM symbol, $y^i[n]$ the received time-domain IFFT sequence of the ith OFDM symbol, and Δt_s the real-valued time difference measured in time sample unit between an IFFT sequence and a sampled sequence. Input of $y^i[n]$ ranges over $n \in [-N_{CP}, N-1]$ and $y^i[n]$ where $n \in [-N_{CP}, -1]$ corresponds to CP. Equation (3) shows that synchronization error Δt_s causes phase drift proportional to Δt_s and k. To deploy this property in building a feature characterizing modulation, two objectives should be addressed: sampling a sequence contained in a single OFDM symbol and removing the phase drift caused by synchronization error.

2.1. Modulation feature extraction

Due to CP, the sequences are repeated at both ends of the symbols in every OFDM symbol. Since both the length of and the distance between repeated sequences are known[1], the position of CP can be found using the autocorrelation,

$$R_{yy}(n,N) = \frac{1}{N_{CP}} \sum_{i=0}^{N_{CP}-1} y[n+i]y^*[n+i+N], \quad (4)$$

which has peaks when n is the first index of CP. To find a peak, we find a sample whose amplitude is larger than both adjacent samples and the minimum distance between two adjacent peaks is set to 90% of OFDM symbol duration, 72-time sample indices. In the sampled sequence, from the remainders of acquired peak-indices divided by OFDM symbol duration, 80, we determine the mode among those remainders as the first index of OFDM symbol, denoted as p.

Due to noise and varying amplitudes of time samples, the estimated CP position might not be accurate. However, our objective is not to find the exact first time sample of the OFDM symbol, but the sequence contained in a single OFDM symbol. Therefore, by sampling the sequence $\{y[p+N_{CP}/2],\ y[p+N_{CP}/2+1],\ \ldots,\ y[p+N_{CP}/2+N-1]\}$, we can sample sequences contained in a single OFDM symbol even though there is a minor error in finding first index of an OFDM symbol.

We have shown that $Y^i_{\Delta t_s}[k]$ is $Y^i[k]$ with phase drift and the amplitude of $Y^i_{\Delta t_s}[k]$ is the same with that of $Y^i[k]$. To remove $\mathrm{e}^{-j2\pi\Delta t_s k/N}$ term in (3), phase differences between the same subcarrier symbols in two consecutive symbol duration are deployed as

$$\Delta\angle Y^i_{\Delta t_s}[k] \triangleq \angle Y^{i+1}_{\Delta t_s}[k] - \angle Y^i_{\Delta t_s}[k]$$
$$= \angle\left\{Y^{i+1}[k]\mathrm{e}^{-j2\pi\Delta t_s k/N}\right\} - \angle\left\{Y^i[k]\mathrm{e}^{-j2\pi\Delta t_s k/N}\right\} \quad (5)$$
$$= \angle Y^{i+1}[k] - \angle Y^i[k].$$

Equation (5) shows that the phase differences between the same subcarrier symbols from sampled sequences are the same as the differences from the received IFFT sequences. Despite the unknown exact Δt_s value, sequences with the same Δt_s can be sampled by setting an interval between starting index of two sample sequences as one OFDM symbol. $|Y_{\Delta t_s}[k]|\mathrm{e}^{j\Delta\angle Y^i_{\Delta t_s}[k]}$ is used as a feature specifying modulation type. In addition, the null subcarrier symbols are

[1] It is assumed that the OFDM parameters are known to the classifier. We leave the estimation of those parameters for future work.

Table 1: DL parameters

Batch size	32	**Loss**	Cross-entropy
Learning rate	$5 \cdot 10^{-5}$	**Epochs**	200

removed by detaching symbols with N_{null} smallest amplitudes. Both cases have been evaluated: with and without null subcarrier symbols.

2.2. CFO correction

To estimate CFO without symbol-level synchronization, we need to use pilot subcarriers as in residual CFO estimation [9] because the preamble is not accessible. To estimate pilot subcarrier indices without a preamble, we use the property that the identical symbols are repeatedly transmitted in pilot subcarriers. The CFO-induced phase difference of pilot subcarrier symbols for adjacent OFDM symbols, $\Delta\angle Y^i_{\Delta t_s}[k]$ is

$$\begin{aligned} Y^i_{\Delta t_s}[k] &= \textstyle\sum_{n=0}^{N-1} y^i[n]\mathrm{e}^{-j2\pi k(n+\Delta t_s)/N} \\ &= \textstyle\sum_{n=0}^{N-1} \left(x^i[n]\mathrm{e}^{-j(2\pi\Delta f_c(n+(i-1)(N+N_{CP}))T_s)}\right)\mathrm{e}^{-j2\pi k(n+\Delta t_s)/N} \\ &= X^i[k+\Delta f_c(N+N_{CP})T_s]\mathrm{e}^{-j(2\pi(\Delta f_c(i-1)(N+N_{CP})T_s+k\Delta t_s/N)} \\ &\approx X^i[k]\mathrm{e}^{-j2\pi(\Delta f_c(i-1)(N+N_{CP})T_s+k\Delta t_s/N)} \\ &\Rightarrow \Delta\angle Y^i_{\Delta t_s}[k_p] = -2\pi\Delta f_c(N+N_{CP})T_s\ , \end{aligned} \tag{6}$$

where k_p denotes the subcarrier index of pilot subcarriers.

For a Wi-Fi link operating at $f_c = 5$ GHz and a frequency tolerance of 1 ppm for commercial-off-the-shelf temperature-compensated crystal oscillators (TXCO) [10] on both sides of the link, the worst-case CFO is $\Delta f_c = 2f_c \cdot 10^{-6} = 10$ kHz. The CFO-induced angular error on $\Delta\angle Y^i_{\Delta t_s}[k_p]$ due to CFO at ± 10 kHz is upper bounded by $10^4 \cdot 80/(20 \cdot 10^6) \cdot 360^\circ \approx 14.4^\circ$. Using those values, $X^i[k + \Delta f_c(N + N_{CP})T_s]$ is approximated to $X^i[k]$ since the worst case $\Delta f_c(N+N_{CP})T_s$ is 0.04, which is much smaller than one, the minimum unit of k. This only works for pilot subcarrier symbols since data subcarrier symbols change randomly with the data bits.

Using the pilot subcarriers' property, CFO is estimated with pilot subcarriers:

$$\begin{aligned} \Delta\angle Y^i_{\Delta t_s}[k] &= -2\pi\Delta f_c(N+N_{CP})T_s \\ \Rightarrow \Delta f_c &= -\Delta\angle Y^i_{\Delta t_s}[k]/(2\pi(N+N_{CP})T_s) \end{aligned} \tag{7}$$

We consider CFO as the average of Δf_c from (7) evaluated at null subcarriers. To correct CFO effect, we multiply time samples $y[n]$ by the term, $\mathrm{e}^{2\pi\Delta f_c n T_s}$ where $n = \{0, 1, 2, \cdots\}$, which is negative of the phase caused by CFO.

2.3. Convolutional neural network

Fig. 2 and Table 1 describe the overall structure of the DL model for the classifier, which is based on CNN. We use four convolutional layers followed by three fully-connected (FC) layers with ReLU as an activation function. Kernel size and stride of each max pooling layer are adaptively chosen by the output shape of each layer. Input is normalized so that the average amplitude of each input subcarrier sample is 1.

Table 2: Data generation parameters

Bandwidth	20 MHz
Carrier frequency	2.4 GHz
SNR	[2, 20] dB in steps of 2 dB
$\{N, N_{CP}\}$	{64, 16}
Input shape	Proposed feature: $2 \cdot (64/52) \cdot 20$ Time IQ: $2 \cdot 1600$ STFT feature: $2 \cdot 5 \cdot 512$

3. EVALUATION

3.1. Evaluation Environments

Simulated and over-the-air (OTA) data are employed in our evaluation with parameters in Table 2 corresponding to Non-HT mode 20 MHz bandwidth Wi-Fi. OTA data are generated with two N310 USRP in OTA transmission settings, see in Fig. 3. The distance between Tx and Rx is 8.84 m. For simulated data, AWGN is utilized as a channel.

One classifier input requires 1600+80+80 samples. The first additional 80 samples are needed since the starting index of an OFDM symbol is unknown. We sample 1680 samples starting from index $i_s \in [0,\ N-1]$, deploying the procedure in Sec. 2. One more OFDM symbol corresponding to the next 80 samples is needed since phase differences between OFDM symbols are used as our features.

For comparison schemes, using raw time IQ samples and complex STFT features as inputs are evaluated. For a fair comparison, the same number of OFDM symbols is used for both inputs. Time IQ samples use 1600 time samples so that the input dimension is $2 \cdot 1600$ (a channel for both real and imaginary). For STFT features, FFT size = 512 and frame overlapping = 50% are deployed as FFT parameters.

3.2. Evaluation results

Fig. 4 shows the classification accuracy performance with simulated data. In every SNR, the proposed feature outperforms the time IQ and STFT feature regardless of symbol-level synchronization. Since the number of modulation classes is four, 25% accuracy achieved with time IQ and STFT without symbol-level synchronization corresponds to that of the uninformed random classifier. Removing the null subcarriers increases classification performance in every case. At 20 dB SNR, it is increased from 89% to 99% by deleting null subcarriers. Both accuracies are higher at 20 dB SNR than the 87% and 79% achieved by [11, 12], both assume symbol-level synchronization and test on simulated data.

Fig. 3b illustrates the accuracy of correctly choosing the first index with the method in Sec. 2 with error, ϵ. The accuracy means that the estimated first sample is at most ϵ time samples away from the ground-truth. In Fig. 3b, accuracy to find the exact first time sample of an OFDM symbol is below 60% at 20 dB SNR, but accuracy accepting at most $N_{CP}/2 = 8$ time samples error is 95% at 2 dB SNR. The sampling method in Sec. 2 lets a sequence contained in a single OFDM symbol reliably sampled even at low SNR.

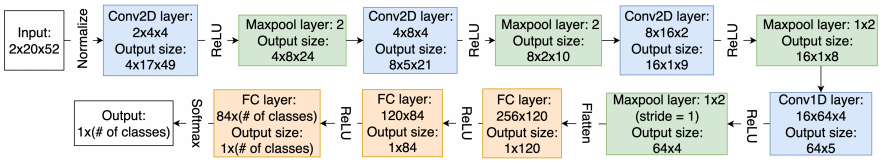

Fig. 2: CNN-based modulation classifier structure.

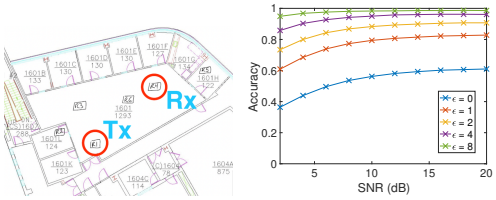

(a) (b)

Fig. 3: (a) The evaluation environment map and (b) Accuracy for choosing the first index of CP with acceptable error ϵ.

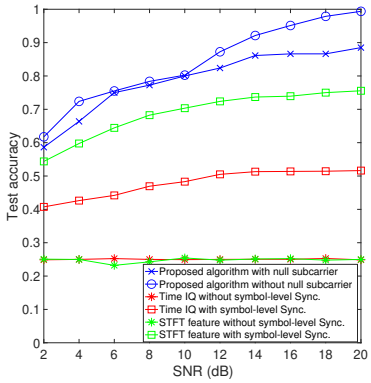

Fig. 4: Test accuracy vs. test data SNR with simulated data.

The proposed algorithm outperforms the case where time IQ samples or STFT features are used on OTA data as well as removing the null subcarrier improves the performance. In particular, at 2 dB SNR and 20 dB SNR, test accuracy is improved from 53 to 59% and 85 to 99%, respectively. Comparing Fig. 5a and Fig. 5c, removing null subcarrier makes the features of 16QAM and 64QAM more distinct at high SNR.

4. RELATED WORK

Many have built DL-based modulation classifier for OFDM signals [11–18] and all of [11–18] have achieved at least 75% classification accuracy at 20 dB SNR. However, none of the studies [11–18] has done the evaluation with hardware-generated data. The algorithm in [13] deploys correlation both within a symbol and among different symbols, thus the classifier knows the exact first indices of OFDM symbols; i.e., symbol-level synchronization. Modulation classifiers has been implemented based on CNN [11, 14, 15] or long short term memory network (LSTM) [12] all with over 80% classification accuracy at 20 dB SNR. Their input comprises time samples for two OFDM symbols after removing CP, which requires the classifier synchronized at the symbol-level. Modulation classifiers in [17, 18] take signals after removing cyclic prefix (CP) and using FFT as an input. Therefore, it is assumed that the classifier is synchronized at the symbol-level. The work in [16] studies modulation classification under multipath channel, but only deals with the single-carrier signals. The authors of [19] classify wireless signals, but recognizes wireless protocols, not modulations.

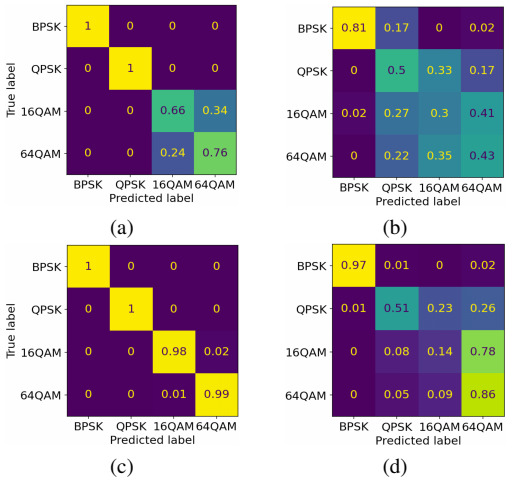

(a) (b) (c) (d)

Fig. 5: Confusion matrices for classification results with OTA data: (a) 20 dB SNR with null subcarrier, (b) 2 dB SNR with null subcarrier, (c) 20 dB SNR after removing null subcarrier, and (d) 2 dB SNR after removing null subcarrier.

There are papers on OFDM modulation classification without symbol-level synchronization based on mathematical modeling [20, 21] without using DL. However, their classifier structure depends on the modulation set, so the structure must be redesigned when classifying signals with a modulation not in the set [20, 21]. Their algorithms [20, 21] can identify OQPSK and MSK, but neither of their evaluations includes high-order QAM like 64QAM, used in practical Wi-Fi.

5. CONCLUSION

OFDM modulation classification is addressed without symbol-level synchronization. We propose a preprocessing for extracting features invariant to synchronization error. Fine-grained preprocessing include the estimated CP position and CFO correction. The proposed CNN-based classifier based on those features classifies the modulation of OFDM in evaluations with simulated and hardware-generated data with maximum 99% classification accuracy at 20 dB SNR. Best test accuracy is achieved by the proposed CNN-based classifier with null subcarrier removal.

6. REFERENCES

[1] J. Gao, X. Yi, C. Zhong, X. Chen, and Z. Zhang, "Deep learning for spectrum sensing," *IEEE Wireless Commun. Lett.*, vol. 8, no. 6, pp. 1727–1730, 2019.

[2] H. Kim, Y. Jiang, S. Kannan, S. Oh, and P. Viswanath, "Deepcode: Feedback codes via deep learning," in *Proc. Adv. Neural Inf. Process. Syst.*, vol. 31, 2018, pp. 9436–9446.

[3] C. Luo, J. Ji, Q. Wang, X. Chen, and P. Li, "Channel state information prediction for 5g wireless communications: A deep learning approach," *IEEE Trans. Netw. Sci. Eng.*, vol. 7, no. 1, pp. 227–236, 2018.

[4] F. Meng, P. Chen, L. Wu, and X. Wang, "Automatic modulation classification: A deep learning enabled approach," *IEEE Trans. Veh. Technol.*, vol. 67, no. 11, pp. 10 760–10 772, 2018.

[5] V. Sathyanarayanan, M. Wagner, and P. Gerstoft, "Over the air performance of deep learning for modulation classification across channel conditions," in *Proc. IEEE Asilomar Conf. Signals, Syst. Comput.*, Nov. 2020, pp. 157–161.

[6] V. Sathyanarayanan, A. Jolly, and P. Gerstoft, "Novel training methodology to enhance deep learning based modulation classification," in *Proc. IEEE Asilomar Conf. Signals, Syst. Comput.*, Oct. 2021, pp. 356–360.

[7] IEEE 802.11ax, "Part 11: Wireless LAN medium access control (MAC) and physical layer (PHY) specifications amendment 1: enhancements for high-efficiency WLAN," May 2021.

[8] A. Kumar, S. Majhi, G. Gui, H.-C. Wu, and C. Yuen, "A survey of blind modulation classification techniques for ofdm signals," *Sensors*, vol. 22, no. 3, p. 1020, 2022.

[9] J. K. Tan, "An adaptive orthogonal frequency division multiplexing baseband modem for wideband wireless channels," Master's thesis, Massachusetts Institute of Technology, 2006.

[10] GTXO-203T | 1.8V∼3.6V SM TCXO | Golledge. [Online]. Available: https://www.golledge.com/products/gtxo-203t-ultra-miniature-tight-stability-tcxo/c-26/p-287/

[11] S. Hong *et al.*, "Deep learning-based signal modulation identification in ofdm systems," *IEEE Access*, vol. 7, pp. 114 631–114 638, 2019.

[12] Z. Zhang, H. Luo, C. Wang, C. Gan, and Y. Xiang, "Automatic modulation classification using cnn-lstm based dual-stream structure," *IEEE Trans. Veh. Technol.*, vol. 69, no. 11, pp. 13 521–13 531, 2020.

[13] T. Huynh-The, Q.-V. Pham, T.-V. Nguyen, X.-Q. Pham., and D.-S. Kim, "Deep learning-based automatic modulation classification for wireless ofdm communications," in *Proc. IEEE ICTC*, Oct. 2021, pp. 47–49.

[14] J. Shi *et al.*, "Deep learning-based automatic modulation recognition method in the presence of phase offset," *IEEE Access*, vol. 8, pp. 42 841–42 847, 2020.

[15] S. Hong *et al.*, "Convolutional neural network aided signal modulation recognition in ofdm systems," in *Proc. IEEE VTC*, May 2020, pp. 1–5.

[16] J. Venalainen, L. Terho, and V. Koivunen, "Modulation classification in fading multipath channel," in *Proc. IEEE Asilomar Conf. Signals, Syst. Comput.*, vol. 2, 2002, pp. 1890–1894.

[17] D. H. Al-Nuaimi, N. A. M. Isa, M. F. Akbar, and I. S. Z. Abidin, "Amc2-pyramid: Intelligent pyramidal feature engineering and multi-distance decision making for automatic multi-carrier modulation classification," *IEEE Access*, vol. 9, pp. 137 560–137 583, 2021.

[18] Z. Zhao, *et al.*, "Modulation format recognition based on transfer learning for visible light communication systems," in *Proc. Optoelectronics Commun. Conf.*, July 2021, p. JS2B.12.

[19] S. R. Shebert, A. F. Martone, and R. M. Buehrer, "Wireless standard classification using convolutional neural networks," in *Proc. IEEE GLOBECOM*, 2021, pp. 1–6.

[20] R. Gupta, S. Kumar, and S. Majhi, "Blind modulation classification for asynchronous ofdm systems over unknown signal parameters and channel statistics," *IEEE Trans. Veh. Technol.*, vol. 69, no. 5, pp. 5281–5292, 2020.

[21] A. K. Pathy, A. Kumar, R. Gupta, S. Kumar, and S. Majhi, "Design and implementation of blind modulation classification for asynchronous mimo-ofdm system," *IEEE Trans. Instrum. Meas.*, vol. 70, pp. 1–11, 2021.